Athens Institute for Education and Research
ATINER

ATINER's Conference Paper Series
ENV2013-0413

Catalytic Activity of Mesoporous SBA-15 modified with Pt and Ti in a Deep Methane, *n*-hexane and CO Oxidation

Hristo Kolev
Assistant professor Dr.
Institute of Catalysis, Bulgarian Academy of Sciences
Sofia, Bulgaria

Silviay Todorova
Associate professor Dr.
Institute of Catalysis, Bulgarian Academy of Sciences
Sofia, Bulgaria

Anton Naydenov
Associate professor Dr.
Institute of General and Inorganic Chemistry,
Bulgarian Academy of Sciences
Sofia, Bulgaria

Ramona Ene
Researcher Dr.
Institute of Physical Chemistry
Bucharest, Romania

Georgi Ivanov
Researcher
Institute of General and Inorganic Chemistry,
Bulgarian Academy of Sciences
Sofia, Bulgaria

Viorica Parvulescu
Professor Dr.
Institute of Physical Chemistry
Bucharest, Romania

Georgi Kadinov
Associate professor Dr.
Institute of Catalysis, Bulgarian Academy of Sciences
Sofia, Bulgaria

An Introduction to
ATINER's Conference Paper Series

ATINER started to publish this conference papers series in 2012. It includes only the papers submitted for publication after they were presented at one of the conferences organized by our Institute every year. The papers published in the series have not been refereed and are published as they were submitted by the author. The series serves two purposes. First, we want to disseminate the information as fast as possible. Second, by doing so, the authors can receive comments useful to revise their papers before they are considered for publication in one of ATINER's books, following our standard procedures of a blind review.

Dr. Gregory T. Papanikos
President
Athens Institute for Education and Research

Catalytic Activity of Mesoporous SBA-15 modified with Pt and Ti in a Deep Methane, *n*-hexane and CO Oxidation

Hristo Kolev
Assistant professor Dr.
Institute of Catalysis, Bulgarian Academy of Sciences
Sofia, Bulgaria

Silviay Todorova
Associate professor Dr.
Institute of Catalysis, Bulgarian Academy of Sciences
Sofia, Bulgaria

Anton Naydenov
Associate professor Dr.
Institute of General and Inorganic Chemistry, Bulgarian Academy of Sciences
Sofia, Bulgaria

Ramona Ene
Researcher Dr.
Institute of Physical Chemistry
Bucharest, Romania

Georgi Ivanov
Researcher
Institute of General and Inorganic Chemistry, Bulgarian Academy of Sciences
Sofia, Bulgaria

Viorica Parvulescu
Professor Dr.
Institute of Physical Chemistry
Bucharest, Romania

Georgi Kadinov
Associate professor Dr.
Institute of Catalysis, Bulgarian Academy of Sciences
Sofia, Bulgaria

Abstract

Ti-SBA-15 composite materials containing 5 and 10% Ti are obtained by direct synthesis (samples denoted Pt Tix) or by impregnation of SBA-15 with titanium isoporopoxide solution (samples denoted i-Tix, x is Ti concentaration). After calcination, the composite Ti-SBA-15 oxides are impregnated with an aqueous solution of a Pt precursor. The as-synthesized samples are characterized by SEM, XRD, XPS and tested in reaction of CO oxidation, n-hexane and methane combustion. XPS results reveal the presence of Pt^+ and Pt^0 on the surface of oxidized Pt Tix sample and strong interaction between Pt^0 and Ti in i-Tix sample. After deposition of Pt on this sample, the finely dispersed Pt metal and Pt_2O are formed on the support. The modification of pure siliceous SBA-15 with titanium by impregnation results in the formation of finely divided TiO_2. Successive introduction of platinum leads to the formation only of Pt^0 with 40 nm particles. The catalysts in which Pt is in a form of large metal particles and TiO_2 is finely dispersed on the support exhibit highest catalytic activity in all studied reactions. The presence of water caused an increase in catalytic activity in CO oxidation and this is more remarkable for impregnated samples.

Keywords: Ti-SBA-15 mesoporous oxide; Pt modified SBA-15, Hydrocarbon oxidation, CO oxidation.

Corresponding Author:

Introduction

Volatile organic compounds (VOC) are recognized as major contributors to air pollution, especially in the low atmosphere of urban and industrial areas. When there is no interest in recovering VOC, they are usually destroyed by deep oxidation. Among the techniques to decompose VOC, catalytic oxidation is preferable to thermal oxidation because of its low energy consumption and lower temperature of operation. The design of a catalytic system for complete oxidation of hydrocarbons is an important problem of the environmental catalysis. It is well known that the complete VOC oxidation catalysts can be classified into three categories: (1) supported noble metals; (2) metal oxides or supported metal oxides; (3) mixtures of noble metal and metal oxides. Major part of the commercial catalysts for VOC destruction belongs to the first category, because the reaction can start at temperature as low as room.

The active phase dispersion in supported catalysts is important for their activity. The following factors influence the active phase dispersion: support type, method of preparation, calcination conditions, precursors and active phase loading. The mesoporous support would give rise to well-dispersed and stable metal particles, supplying abundant pores and large surface area, thus possessing a great potential in further improvement of the catalytic performance. Among the different types of mesoporous silicas, SBA-15 supports have attracted much interest because of their thicker pore walls and higher hydrothermal stability compared to MCM-41 materials (Zhao *et al.*, 1998).

The synthesis of mesostructured TiO_2 with high surface area has attracted much scientific and technological attention due to its numerous applications (catalysis, photocatalysis and photovoltaics, electrochronics and sensors, etc.) (Bonne *et al.*, 2010; Grätzel, 2001; Hagfeldt & Grätzel, 1995; Linsebigler *et al.*, 1997). The thermal stability of pure mesoporous titanium oxide remains low, and calcination results in the collapse of the pore structure. The heating at temperatures above 450°C leads to the transition anatase to rutile (Zhang & Banfield, 1998). The phase transition is associated with an increase in crystal size, and therefore in a drastic decrease in surface area. To overcome these drawback different methods for TiO_2 deposition on mesostructured SiO_2 support were proposed. The synthesis routes include titanium impregnation/grafting (Anderson *et al.*, 2001; Bonne *et al.*, 2010; Bonne *et al.*, 2010), titanium incorporation in silica framework (Ungureanu *et al.*, 2008), or incorporation of preformed titania nanoparticles (Fattakhova-Rohlfing *et al.*, 2009).

Platinum based materials have gained a significant interest due to their high efficiency as catalysts in some important environment processes, such as oxidation of CO and VOC (Tsou *et al.*, 2005; Spivey, 1987), PROX (Teschner *et al.*, 2007; Wu *et al.*, 2000), DeNox *et al (2011).* (Olympiou & Efstathiou, 2011). High dispersion of precious metal particles on the support is important for the enhancement of the catalytic activity as well as for the reduction in the cost of catalyst materials. It was established that modification of alumina

(Solange de Resende *et al.*, 1999) or SBA-15 (Wang *et al.*, 2004) with titanium led to the increase in Pt dispersion of and as consequence the catalytic activity. The combination of the finely dispersed Pt with high thermal stability of SBA-15 could lead to the catalysts with high activity and stability.

The main object of this study is the effect of preparation method of Pt xTiSBA-15 catalysts on the catalytic activity in CO oxidation and *n*-hexane and methane combustion. These three compounds are among major air pollutants. Hexane is a component of many products related to industry. In the atmosphere it participates in radical reactions, yielding 2-hexanone, 2- and 3-hexyl nitrate and 5-hydroxy-2-pentanone, all of them existing in the photochemical smog. Methane is a by-product formed in several industrial processes, and a major hydrocarbon air pollutant received from natural gas fuelled vehicles and gas power plants. Methane has a much larger detrimental greenhouse effect than carbon dioxide.

2. Sample preparation

The Ti-SBA-15 composite materials with 5 and 10 % Ti content are obtained by direct synthesis (samples denoted Tix, x is Ti concentration) or by impregnation of SBA-15 with titanium isoporopoxide solution (i-Tix). In the first method the amphiphilic triblock copolymer (Pluronic P123 with average molecular weight 5800) was dispersed in 1.6 M HCl aqueous solution with stirring at 313 K for 24 hours. Tetraethylorthosilicate and titanium isoporopoxide dissolved in isopropyl alcohol were added in the obtained homogeneous solution and the obtained mixture was kept at the same temperature another 24 h. The gel with molar composition 1.0 TEOS: 0.1 P123:x TiO_2 :0.1 HCl:850 H_2O (where x=0 for SBA-15, and x=0.4 for Ti-SBA-15) is then hydrothermally treated in a Teflon-lined autoclave at 373 K for 2 days. The resulting solid was centrifuged, filtered, washed with deionized water, and dried in air at room temperature. The calcination of the as-synthesized samples was performed at 823 K under air flow for 8 hours.

In order to prepare i-Tix sample, the SBA-15 material was impregnated with solution of titanium isoporopoxide in isopropyl alcohol, dried and calcined 6 h at 823 K. Platinum was introduced by impregnation with aqueous H_2PtCl_4 solution and calcined 6h at 823 K. Platinum loading in the final material is 0.25 %.

3. Sample characterization

Powder XRD patterns are collected at room temperature in a step-scan regime (step=0.05º, count time = 2 s) on Bruker AXS diffractometer using CuK_α radiation (λ = 1.5718 Å). XRD data processing is performed by using the X'Pert HighScore program. SEM images are recorded with a Zeiss-Evo LS10 scanning electron microscope.

The XPS measurements are carried out in the UHV chamber of an ESCALAB-MkII (VG Scientific, now Thermo Scientific) electron spectrometer with a base pressure of about 1×10^{-10} mbar (during the

measurement 1×10^{-9} mbar) at room temperature. The photoelectron spectra are obtained using unmonochromatized AlKα (hν=1486.6 eV) radiation. Passing through a 6-mm slit (entrance/exit) of a hemispherical analyzer, electrons with energy of 20 eV are detected by a channeltron. Because of the small signal for Pt4f, 50 eV pass energy is used. The instrumental resolution, measured as the full width at half maximum (FWHM) of the $Ag3d_{5/2}$ photoelectron peak is about 1 eV. The energy scale is corrected to the Si2p-peak maximum at 103.3 eV for electrostatic sample charging. The recorded XPS spectra are performed, using a symmetrical Gauss-Lorentzian curve fitting after Shirley-type subtraction of the background (Shirley, 1972).

4. Catalytic tests

Catalytic activity tests were performed using an integrated quartz micro-reactor and mass spectrometer system (CATLAB, Hiden Analytical, UK). The system features a fast-response, low thermal mass furnace with integrated air-cooling, a precision Quadrupole Mass Spectrometer, and a quartz inert capillary with 'hot zone' inlet for continuous close-coupled catalyst sampling with minimal dead volume and memory effects. The reactant gases were supplied through electronic mass flow controllers. The catalysts (particles size of 0.3-0.6 mm) were held between plugs of quartz wool in a quartz tubular vertical flow reactor (Ø = 6 mm). An inlet concentration of CO, *n*-hexane and methane in air were 600, 840 and 900 ppm respectively. External mass transfer limitations have been minimized by working at high GHSV (30 000 h^{-1}).

5. Results and discussion

Powder X-ray diffractograms of all studied catalysts are shown in Figure 1. The broad single pattern present in all diffractograms is caused by the amorphous silica walls of the SBA-15 material. The low resolved peak at 2θ = 33.4 visible in spectra of Pt Ti10 is ascribed to the PtO (PDF 00-043-1100). The X-ray patterns of Pt i Ti5 and Pt i Ti10 contain lines only for metal platinum. The mean Pt particles size calculated according to Scherrer equation is 40 nm for Pt i Ti10 and 35 nm for Pt i Ti5. The absence of diffraction lines for TiO_2 reveals its fine dispersion. Anatase and rutile crystalline phases are detected by XRD in the sample obtained by direct synthesis (Pt Ti5 and Pt Ti10). The fiber type morphology obtained for SBA-15 (Figure 2A) is slightly modified after Pt and Ti impregnation. A slight change in morphology is evidenced for Pt-i-Ti sample (Figure 2B). Smaller fibers like roads are evidenced by SEM microscopy for these samples. The homogeneity is affected for the samples obtained by direct synthesis. A mixture of bars scattered among particles with a variety of forms and sizes is obtained. These images support XRD results, indicating rapid precipitation of titanium hydroxide in aqueous medium with low pH during SBA-15 synthesis. Surfactant dispersion in the aqueous medium favors the formation, after calcination, of two titania systems (anatase, rutile) evidenced by XRD (Figure 1). UV-Vis spectra shown, for i-Ti-SBA-15 sample, a band at about 250 nm characteristic for the charge-transfer transition associated with regular $Ti^{4+}O_4$ framework tetrahedral (Medina-Mendoza *et al.*, 2011). The formation of titanium crystals species in Ti-SBA-

15 species is evidenced by the band to higher wavelengths (around 330 nm) (Moulder *et al.*, 1992).Small angles (Figure 3) diffraction peaks of the hexagonal mesopore structure are observed in cases of sample with 5% titania showing that this concentration do not affect the pore structure. The destruction of the ordered structure is visible for 10wt% Ti concentration.

The detailed XP spectra are needed to understand the oxidation states of the different Pt nanoparticles obtained by the different preparation methods. Figure 4 shows the high-resolution XP spectra of Pt4f region. The obtained binding energies for a sample prepared by direct synthesis are 70.5 and 72.8 eV. These binding energies are measured as well as for the samples with 10% Ti content and 5% Ti content. They are ascribed to the Pt^0 from platinum particles and Pt^+ in Pt_2O, respectively (Medina-Mendoza *et al.*, 2011; Moulder *et al.*, 1992). Comparing the spectra form used and unused samples we can conclude that there is no difference in the oxidation states in platinum. Nevertheless, there are some changes in the concentration ratio Pt^+/Pt^0, which is 0.3 for the unused catalyst and changes to 0.8 for the used sample, respectively. When the platinum is deposited on SBA-15 modified by impregnation with titanium source, the measured binding energy for $Pt4f_{7/2}$ is at 71.5 eV and could be ascribed to the Pt^0 strongly interacting with TiO_2 or possible formation of Pt_3Ti alloy. As one can see the oxidation state of Pt does not change after reaction, but we observe reduction of the platinum concentration (Table 1). This can be explained with covering platinum particles with titania during the catalytic reaction.

The formation of Pt_3Ti is very unlikely under the conditions used for the synthesis of this sample. Moreover, the obtained binding energies for Ti2p peak (Figure 5), for the samples prepared by impregnation of SBA-15 with titanium isopropoxide solution, are 458.1 eV and 459.1 eV, respectively. These binding energies, of the curve fitted Ti2p peak with two subpeaks, are ascribed to Ti^{4+} in TiO_2 particles, which are finely dispersed and interact respectively weaker or stronger with the substrate. The particles strongly interacting with support predominate. Therefore, we can exclude the formation of Pt_3Ti alloy. For the other samples, prepared by direct synthesis, the obtained binding energy for Ti2p peak is about 457.3 eV, which is ascribed to Ti in a TiO_2 bulk phase. Again, there are no major differences in the oxidation states of Ti for the measured samples before and after reaction (unused and used). A closer look of curve fitted high resolution spectra reveals change in the $Ti^{4+}(TiO_2$ particles)/$Ti^{4+}(TiO_2$ bulk phase) ratio. This ratio is calculated to be 4.67 for the unused sample Pt I Ti10 before reaction and 0.79 for the used sample Pt I Ti10 after reaction, respectively. This, of course, means an enormous increase of the TiO_2 bulk phase on the surface of the sample, which is one more sign of the above mentioned covering platinum particles with titanium during the catalytic reaction.

The temperature dependences of the CO oxidation and *n*-hexane and methane combustion over all prepared catalysts are shown in Figures 6. H_2O and CO_2 were the only detectable reaction products in *n*-hexane and methane oxidation on all investigated samples. The tested catalysts exhibit very low

catalytic activity is methane combustion. A catalyst that often has been used for methane oxidation is palladium supported on Al_2O_3. Burch *et al. (1994)* (Burch & Loader, 1994) showed that Pt/ alumina catalyst is a more efficient catalyst than is Pd/ alumina catalyst for high conversions of methane in the cases of stochiometric or rich mixtures. Our catalytic experiment shows that the catalytic system Pt-Ti-SBA-15 is not suitable for reaction of the complete methane oxidation.

The order of activity *n*-hexane and CO oxidation is as follows: Pt i Ti10 > Pt Ti10 > Pt i Ti5 > Pt Ti5. The most active catalyst is Pt i Ti10 in which Pt is in a form of large metal particles and TiO_2 is finely dispersed on the support. The reduced metallic Pt clusters are considered the active centres for catalytic oxidation of hydrocarbons (Völter *et al.*, 1987). It has been reported that oxidation of volatile organics catalysed by noble metals undergoes the dissociative adsorption of oxygen first, followed by direct reaction of the dissociated oxygen with the reactant (Spivey, 1987)

The activity of the samples in *n*-hexane oxidation dropped during time on stream. The decrease in the catalytic activity cannot be correlated only with sintering of the Pt particles. Particle size calculations according to XRD data on spent samples demonstrate about a three-fold increase in the mean particle diameter of the Pt in Pt Ti10 during the stability test. There is a not change in the mean particle size of other samples (Table 1). As was mentioned above the metallic Pt particles are active centers for hydrocarbon oxidation. The ratio Pt^+/Pt^0 increases in the used catalysts as was demonstrated by XPS. The formation of platinum oxides during the reaction could be responsible for decrease in activity in time on stream.

A very interesting phenomenon was observed during CO oxidation in the presence of H_2O. The water caused an increase in catalytic activity and this is more remarkable for impregnated samples. It has been found that conversion of CO at low temperatures (<300°C) is significantly improved when Pt is dispersed on TiO_2 samples of low crystallite size (Panagiotopoulou, P., Kondarides, D. I., 2004). Our results are with accordance with this statement. It was demonstrated that the modification of pure siliceous SBA-15 with titanium by impregnation results in the formation of two types finely divided TiO_2 on SBA-15 support.

5. Conclusion

The state of platinum in the titanium modified SBA-15 depends very much of the method of Ti introduction. When Ti is introduced by direct synthesis in the starting gel, the titanium in the final materials is well crystalline rutile and anatase. After deposition of platinum by impregnation and next calcinations the finely dispersed Pt metal and Pt_2O are formed on the support.

The modification of pure siliceous SBA-15 with titanium by impregnation results in the formation of two types finely divided TiO_2 on SBA-15 support – less and strong interacting with the framework of SBA-15. The

introduction of platinum on this sample leads to the formation only of metal Pt with mean diameter 40 nm.

The catalysts in which Pt is in a form of large metal particles and TiO_2 is finely dispersed on the support exhibit higher catalytic activity in all studied reaction. The presence of water caused an increase in catalytic activity in CO oxidation and this is more remarkable for impregnated samples.

Acknowledgements

References

Anderson, C., Bard, A.J. (1995). 'An Improved Photocatalyst of TiO2/SiO2 Prepared by a Sol-Gel Synthesis.' *J. Phys. Chem., 99*, 9882-9885.

Bonne, M., Pronier, S., Batonneau, Y., Can, F., Courtois, X., Royer, S., Marécot, P., Duprez, D. (2010). 'Surface properties and thermal stability of SiO2-crystalline TiO2 nano-composites.' *J. Mater. Chem., 20*, 9205-9214.

Bonne, M., Pronier, S., Can, F., Courtois, X., Valange, S., Tatibouët, J.-M., Royer, S., Marécot, P., Duprez, D. (2010). 'Synthesis and characterization of high surface area TiO2/SiO2 mesostructured nanocomposite.' *Solid, 12*, 1002-1012.

Bonne, M., Samoila, P., Ekou, T., Especel, C. , Epron F., Marécot, P., Royer, S., Duprez,D. (2010). 'Control of titania nanodomain size as a route to modulate SMSI effect in Pt/TiO2 catalysts.' *Cat. Comm., 12*, 86-91.

Burch, R. and Loader, P.K. (1994). 'Investigation of Pt/ Al2O3 and Pd/ Al2O3 catalysts for the combustion of methane at low concentrations.' *Applied Catalysis B: Environmental, 5*(1-2), 149-164.

Chun,H., Yizhong, W., Hongxiao, T. (2001). Preparation and characterization of surface bond-conjugated TiO2/SiO2 and photocatalysis for azo dyes. *Appl. Catal. B, 30*, 277-285.

Fattakhova-Rohlfing, D., Szeifert, J.M., Yu, Q., Kalousek, V., Rathousk, J., Bein, T. (2009). 'Low-Temperature Synthesis of Mesoporous Titania−Silica Films with Pre-Formed Anatase Nanocrystals.' *Chem. Mater., 21*, 2410-2417.

Grätzel, M. (2001). 'Photoelectrochemical cells.' *Nature, 414*, 338-342.

Hagfeldt, A., Grätzel, M. (1995). 'Light-Induced Redox Reactions in Nanocrystalline Systems.' *Chem. Rev., 95*, 735-758.

Linsebigler, A. L., Guangquan. Lu, Yates, J. T. (1995). 'Photocatalysis on TiO2 Surfaces: Principles, Mechanisms, and Selected Results.' *Chem. Rev., 95*(3), 735-758.

Medina-Mendoza, A. K., Cortés-Jácomeb, M. A., Toledo-Antoniob, J. A., Angeles-Chávezb, C., López-Salinas, E., Cuauhtémoc-López, Barrera, M. C., Escobar, J., Navarrete, J., Hernández, I. (2011). 'Highly dispersed uniformly sized Pt nanoparticles on mesoporous Al-SBA-15 by solid state impregnation.' *Appl.Catal. B, 106*, 14–25.

Millis, A.,Le Hunte, S. (1997). 'An overview of semiconductor photocatalysis.' *J. Photochem. Photobiol. A, 108*, 1-35.

Moulder, F., Sticke, W. F., Sobol, P. E., Bombel, K. D. (1992). '*Handbook of X-ray Photoelectron Spectroscopy*' (Vol. Second edition). (J. Castain, Ed.) Minnesota, USA: Perkin-Elmer Corporation, Physical Electron Division.

Olympiou, G. G., Efstathiou, A. M. (2011). 'Industrial NOx control via H2-SCR on a novel supported-Pt nanocatalyst.' *Chem. Engin. J., 170*, 424-432.

Panagiotopoulou, P., Kondarides, D. I. (2004). 'Effect of morphological characteristics of TiO2-supported noble metal catalysts on their activity for the water–gas shift reaction.' *J. Catal., 225*, 327-336.

Shirley, D. (1972). 'High-Resolution X-Ray Photoemission Spectrum of the Valence Bands of Gold.' *Phys. Rev. B, 5*, 4709-4714.

Solange de Resende, N., Eon, J.-G., and Schmal, M. (1999). ,Pt–TiO2–γ Al2O3Catalyst: I. Dispersion of Platinum on Alumina-Grafted Titanium Oxide.' *J. Catal., 183*, 6-13.

Spivey, J. (1987). 'Complete catalytic oxidation of volatile organics.' *Ind. Eng. Chem. Res., 26*, 2165-2180.

Teschner, D., Wootsch, A., Pozdnyakova-Tellinger, O., Kröhnert, J., Vass, E.M., Hävecker, M., Zafeiratos, S., Schnörch, P., Jentoft, P.C., Knop-Gericke, A., Schlögl, R. (2007). ,Partial pressure dependent in situ spectroscopic study on the preferential CO oxidation in hydrogen (PROX) over Pt/ceria catalysts.' *J. Catal., 249*, 318–327.

Tsou, J., Magnoux, P., Guisnet, M., Órfão,J.J.M., Figueiredo, J.L. . (2005). 'Catalytic oxidation of volatile organic compounds: Oxidation of methyl-isobutyl-ketone over Pt/zeolite catalysts.' *Appl. Catal. B, 57*, 117–123.

Ungureanu, A., Drăgoi, B., Chirieac, A., Catrinescu, C., Dumitriu, E. (2008). 'Synthesis of highly ordered titanium-containing SBA-15 mesoporous silicas for catalytic eco-friendly oxidations.' *Env. Eng. Manag. J., 7*, 255-261.

Völter, J., Lietz, G., Spindler, H., Lieske, H. (1987). ,Role of metallic and oxidic platinum in the catalytic combustion of n-heptane.' *J. Catal., 104*, 375-380.

Wang, X., Landau, M. V., Rotter, H., Vradman, L., Wolfson, A., Erenburg, A. (2004). ,TiO2 and ZrO2 crystals in SBA-15 silica: performance of Pt/TiO2(ZrO2)/SBA-15 catalysts in ethyl acetate combustion.' *J. Catal., 222*, 356-571.

Wu, J.C.-S. , Lin, Z., Pan, J., Rei, M. (2000). ,A novel boron nitride supported Pt catalyst for VOC incineration.' *Appl. Catal., A, 219*, 117-124.

Zhang, H., Banfield, J.F. (1998). 'Thermodynamic analysis of phase stability of nanocrystalline titania.' *J. Mater. Chem., 8*(9), 2073-2076.

Zhao, D., Feng, J., Huo, Q., Melosh, N., Fredrickson, G. H., Chmelka, B. F., Stucky, G. D. (1998). 'Triblock Copolymer Syntheses of Mesoporous Silica with Periodic 50 to 300 Angstrom Pores.' *Science, 279*, 548-552.

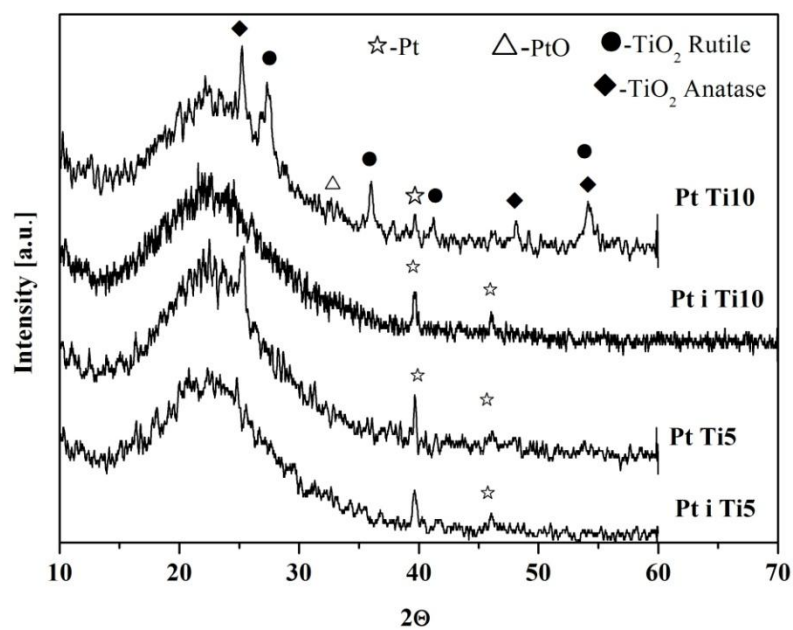**Figure 1.** *XRD patterns of all platinum catalysts after calcinations at 823 K.*

Figure 2. *SEM image of samples A. pure SBA-15 and B. Pt i 5Ti*

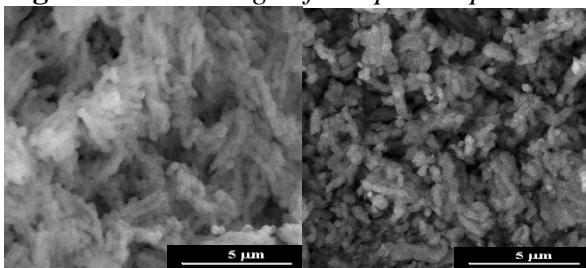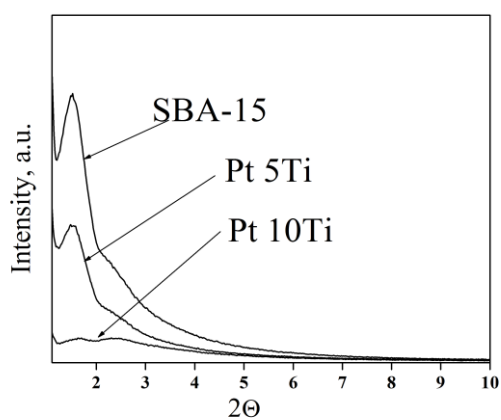**Figure 3.** *Small angle of samples prepared by direct synthesis*

Figure 4. *XP spectra of Pt4f region. Left column shows XP spectra of Pt4f for sample with 10% Ti content, whereas the right column is for the sample with 5% Ti content. The vertical dashed lines are for the orientation of the reader.*

Figure 5. *XP spectra of Ti2p region. Left column shows XP spectra of Ti2p for sample with 10% Ti content, whereas right column is for the sample with 5% Ti content. The vertical dashed lines are for the orientation of the reader.*
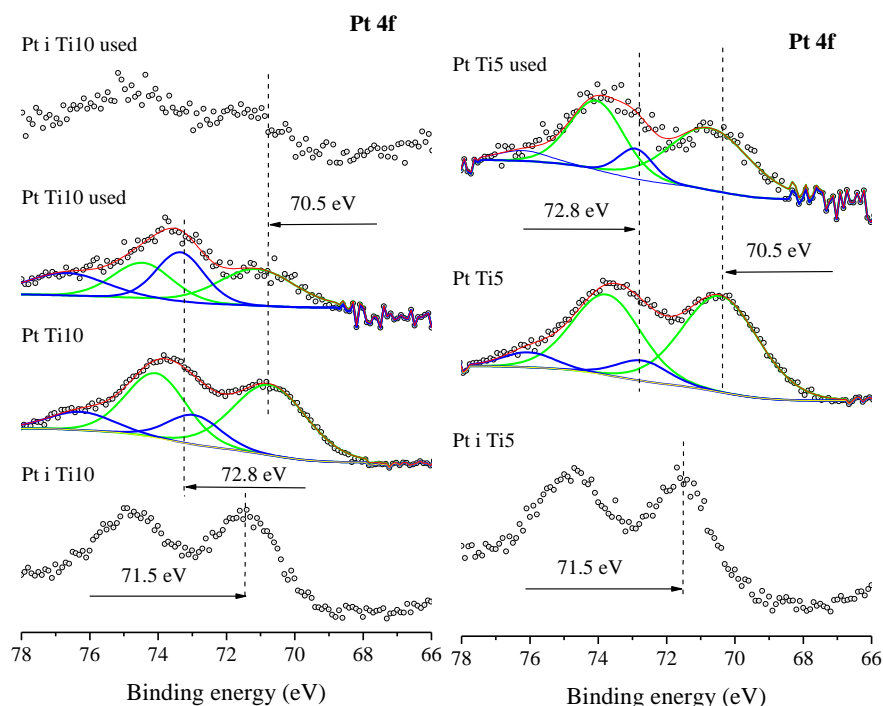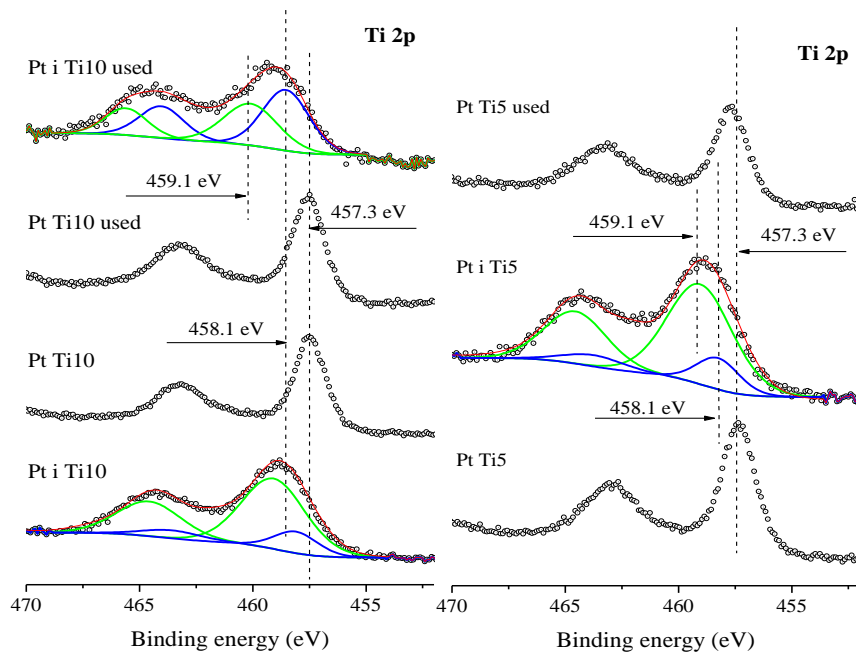

16

Table 1. *XRD particle size and XPS surface atomic concentrations (at. %) of measured samples before reaction (unused) and after reaction (used).*

Samples	D_{pt}, nm according XRD		Atomic percent and Pt/Ti ratio on the surface before reaction, according XPS			Atomic percent and Pt/Ti ratio on the surface after reaction, according XPS		
	unused	used	Pt	Ti	Pt/Ti	Pt	Ti	Pt/Ti
Pt i Ti5	35	-	0.03	1.8	0.016			
Pt Ti5	35	35	0.11	3.0	0.037	0.05	1.67	0.03
Pt i Ti10	40	40	0.04	2.2	0.018	0.01	1.72	0.0058
Pt Ti10	4-5	17	0.11	3.2	0.034	0.05	2.43	0.02

D_{pt} –mean particle size

Figure 6. *Conversion vs. temperature in the reaction of A. complete methane oxidation; B. complete n-hexane oxidation; C. CO oxidation*

A.   B.   C.